Supporting Information for

Flexible Polydimethylsiloxane Composite with Multi-Scale Conductive Network for Ultra-Strong Electromagnetic Interference Protection

Jie Li[1], He Sun[1], Shuang-Qin Yi[1], Kang-Kang Zou[2], Dan Zhang[1], Gan-Ji Zhong[1], Ding-Xiang Yan[2, *], and Zhong-Ming Li[1, *]

[1] College of Polymer Science and Engineering, State Key Laboratory of Polymer Materials Engineering, Sichuan University, Chengdu 610065, P. R. China

[2] School of Aeronautics and Astronautics, Sichuan University, Chengdu 610065, P. R. China

*Corresponding authors. E-mail: yandingxiang@scu.edu.cn (D. X. Yan), zmli@scu.edu.cn (Z. M. Li)

Supplementary Tables and Figures

Table S1 Calculation of the filler contents for PAAC composites

Sample	CNT (vol%)	AAF (vol%)	Ag (vol%)	AAF (wt%)	Ag (wt%)	CNT (wt%)
PAA0C1	1.0	0	0	0	0	1.7
PAA0C2	2.0	0	0	0	0	3.4
PAA0C3	3.0	0	0	0	0	5.1
PAA1C0	0	1.0	0.13	2.6	1.4	0
PAA3C0	0	3.0	0.39	7.5	4.0	0
PAA5C0	0	5.0	0.66	12.2	6.4	0
PAA1C1	1.0	1.0	0.13	2.6	1.3	1.7
PAA3C1	1.0	3.0	0.39	7.5	3.9	1.7
PAA5C1	1.0	5.0	0.66	12.1	6.4	1.6
PAA1C2	2.0	1.0	0.13	2.5	1.3	3.4
PAA3C2	2.0	3.0	0.39	7.4	3.9	3.3
PAA5C2	2.0	5.0	0.66	12.0	6.3	3.2
PAA1C3	3.0	1.0	0.13	2.5	1.3	5.1
PAA3C3	3.0	3.0	0.39	7.4	3.9	4.9
PAA5C3	3.0	5.0	0.66	11.9	6.3	4.8

According to the calculated mass fraction of Ag, the AAF, Ag and CNT contents were respectively calculated based on Eqs. S1-S6 as follows:

$$v_{CNT} = \frac{W_{CNT}/\rho_{CNT}}{W_{AAF}\times\frac{w_{Ag1}}{\rho_{Ag}}+W_{AAF}\times\frac{(1-w_{Ag1})}{\rho_{PLASF}}+\frac{W_{CNT}}{\rho_{CNT}}+\frac{W_{PDMS}}{\rho_{PDMS}}}\times 100\% \quad \text{(S1)}$$

$$v_{AAF} = \frac{W_{AAF}\times\frac{w_{Ag1}}{\rho_{Ag}}+W_{AAF}\times\frac{(1-w_{Ag1})}{\rho_{PLASF}}}{W_{AAF}\times\frac{w_{Ag1}}{\rho_{Ag}}+W_{AAF}\times\frac{(1-w_{Ag1})}{\rho_{PLASF}}+\frac{W_{CNT}}{\rho_{CNT}}+\frac{W_{PDMS}}{\rho_{PDMS}}}\times 100\% \quad \text{(S2)}$$

$$v_{Ag} = \frac{W_{AAF}\times w_{Ag1}/\rho_{Ag}}{W_{AAF}*\frac{w_{Ag1}}{\rho_{Ag}}+W_{AAF}\times\frac{(1-w_{Ag1})}{\rho_{PLASF}}+\frac{W_{CNT}}{\rho_{CNT}}+\frac{W_{PDMS}}{\rho_{PDMS}}}\times 100\% \quad \text{(S3)}$$

$$w_{Ag2} = \frac{W_{AAF}\times w_{Ag1}}{W_{AAF}+W_{CNT}+W_{PDMS}}\times 100\% \quad \text{(S4)}$$

$$w_{AAF} = \frac{W_{AAF}}{W_{AAF}+W_{CNT}+W_{PDMS}}\times 100\% \quad \text{(S5)}$$

$$w_{CNT} = \frac{W_{AAF}}{W_{AAF}+W_{CNT}+W_{PDMS}}\times 100\% \quad \text{(S6)}$$

Where W_{AAF}, W_{CNT}, W_{PDMS} were the calculated weight of AAF, CNT and PDMS; ρ_{Ag}, ρ_{PLASF}, ρ_{CNT}, ρ_{PDMS} were the density of Ag, PLASF, CNT and PDMS; w_{Ag1}, w_{Ag2}, w_{AAF}, w_{CNT} were the mass fraction of Ag in the AAF, and Ag, AAF, CNT in the PAAC composites; v_{Ag}, v_{AAF}, v_{CNT} were the volume content of Ag in the AAF, and Ag, AAF, CNT in the PAAC composites; respectively. The densities of Ag, PLASF and CNT are 10.49, 1.24 and 1.75 g/cm^3.

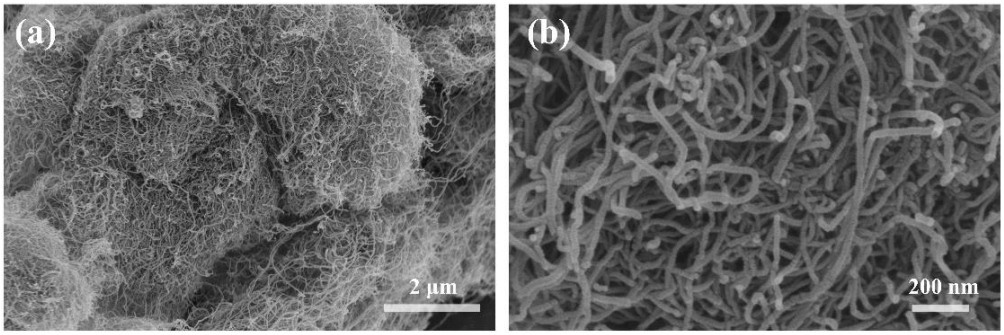

Fig. S1 a, b SEM images of CNT with different magnifications

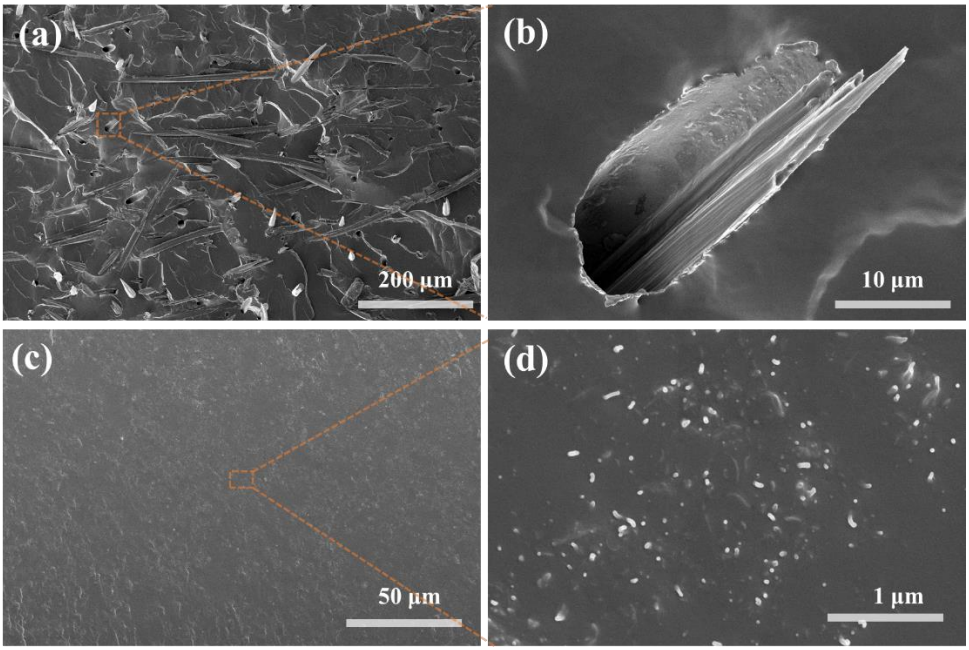

Fig. S2 SEM images of **a, b** PAA5C0 and **c, d** PAA0C3 with different magnifications

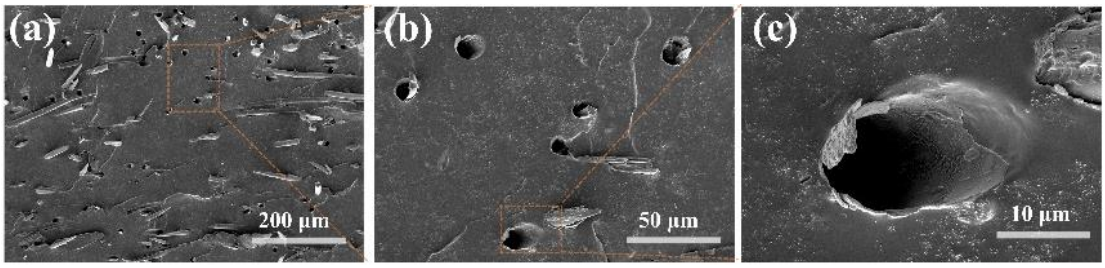

Fig. S3 a-c SEM images of PAA5C3 composites with different magnifications.

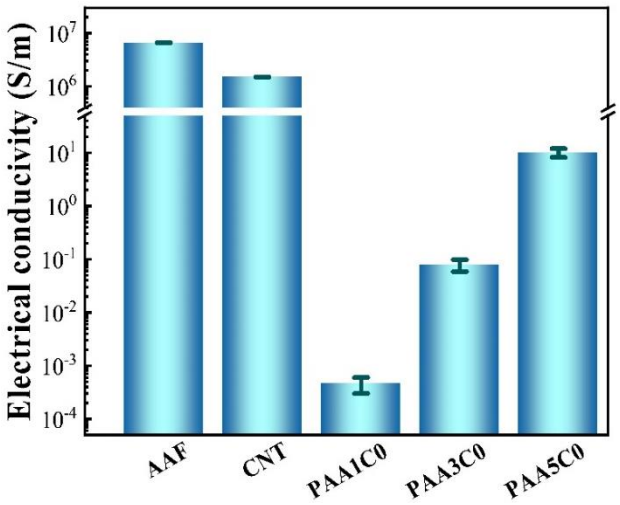

Fig. S4 The electrical conductivity of AAF, CNT and PAAxC0 composites

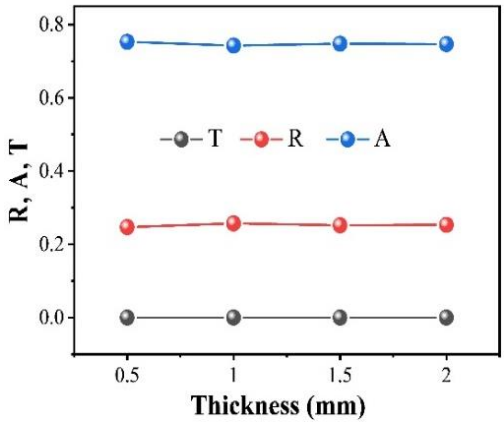

Fig. S5 The reflection coefficient (R), absorption coefficient (A) and transmission coefficient (T) at 10.0 GHz of PAA5C3 composites at different thicknesses

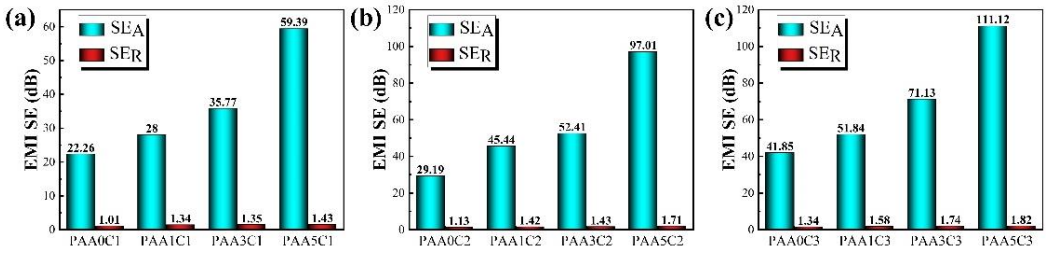

Fig. S6 The absorption loss (SE_A) and reflection loss (SE_R) of **a** PAAxC1, **b** PAAxC2, **c** PAAxC3 composites at the frequency of 10.0 GHz

Table S2 The compression stress and modulus of PAA5C2 composite at different strains

Compression strain (%)	Compression stress (MPa)	Compression modulus (MPa)
10	0.68	66.2
20	1.49	77.7
30	2.50	89.1
40	4.04	139.9
50	6.56	230.0
60	10.68	386.0
70	16.08	543.5
80	23.21	727.4

Table S3 Comparison of other EMI shielding composites in recent 5 years

Sample	Content (wt%)	Thickness (mm)	EMI SE (dB)	Frequency (GHz)	Refs.
PDMS/CNT/Ag	11.1	2	113	8.2-12.4	
PDMS/CNT/Ag	9.5	2	82	8.2-12.4	This
PDMS/CNT	5.1	2	43	8.2-12.4	work
PDMS/Ag	6.4	2	36	8.2-12.4	
PDMS/CNT/GNP	20	3.6	66	8.2-12.4	[S1]
PDMS/CNT/Carbon aerogel	2	2	20	8.2-12.4	[S2]
PDMS/Au@CNT/SA	6	2	60	8.0-12.0	[S3]
PDMS/CNT/Ag	17	4	90	8.2-12.4	[S4]
PDMS/CNT/Ag	17	1.5	56	8.2-12.4	[S4]
PDMS/CNT/TSM	6	2	47.8	8.2-12.4	[S5]
PDMS/Graphene	1.5	4.8	45	8.2-12.4	[S6]
PDMS/HOGF	21.46	5	96	8.2-12.4	[S7]
PDMS/Fe_3O_4-$Ti_3C_2T_X$/GF	11.53	1	83.6	8.2-12.4	[S8]
SEBS/CNT/GNP	10	3	23.3	8.2-12.4	[S9]
SEBS/CNT/GNP	90	2	25	8.2-12.4	[S10]
WPU/CNT	76.2	2.3	35	8.2-12.4	[S11]
PLA/Ag	34.44	1.5	50	8.2-12.4	[S12]
PP/CNT/CB	5	2.5	20	8.2-12.4	[S13]
WPU/Fe_3O_4@rGO/CNT	41.2	0.8	35.9	8.2-12.4	[S14]
PVDF/CNT/MXene	12	0.2	12.6	18-26	[S15]
PANI/rGO/γ-Fe_2O_3	100	2.5	51	8.2-12.4	[S16]
Paraffin/MXene/Ag	60	1	62.7	8.2-18	[S17]
epoxy/CuNWs-TAGA	7.2	3	47	8.2-12.4	[S18]
PC/EMA-GCNT	10	2	34	8.2-12.4	[S19]
PVDF/CNT/rGO- $FeCo_2$	13	3	30	8.2-18	[S20]
PA6/EG/Ni	5.9	2	77.3	8.2-12.4	[S21]
Polyborosiloxane/MS/MXene	22.75	4	37	8.2-12.4	[S22]
TPU/CNTs/Ni@CNT	20	2	69.9	8.2-12.4	[S23]
PVDF/CNT/Ni	7	0.6	57.3	18-26	[S24]
PMMA/MWCNT/GNP	12	2	36	8.0-12.0	[S25]
Ecoflex/LM	67.2	2	81.6	8.2-12.4	[S26]

* GNP, SA, TSM, HOGF, GF, SEBS, WPU, PLA, PP, CB, rGO, PVDF, MXene,]PANI, CuNWs, TAGA, PC, EMA, GCNT, PA6, EG, MS, TPU, PMMA and LM represent graphene nanoplates, sodium alginate, temperature-sensitive microspheres, highly oriented graphite frameworks, graphene foam, poly (styrene-b-ethylene-ran-butylene-b-styrene), waterborne polyurethane, poly(lactic acid), polypropylene, carbon black, reduced graphene oxide, poly(vinylidene fluoride), metal carbides/nitrides/ carbonitrides, polyaniline, copper nanowires, thermally annealed graphene aerogel, polycarbonate, ethylene-methyl acrylate, Graphene-MWCNT hybrid filler, polyamide 6, expanded graphite, melamine sponge, thermoplastic polyurethane, polymerizable ionic liquid copolymer, polymethyl methacrylate and liquid metal, respectively.

Supplementary References

[S1] Q. Wei, S. Pei, X. Qian, H. Liu, Z. Liu et al., Superhigh electromagnetic interference shielding of ultrathin aligned pristine graphene nanosheets film. Adv. Mater. **32**(14), e1907411 (2020). https://doi.org/10.1002/adma.201907411

[S2] M. Chen, L. Zhang, S. Duan, S. Jing, H. Jiang et al., Highly conductive and flexible polymer composites with improved mechanical and electromagnetic interference shielding performances. Nanoscale **6**(7), 3796-3803 (2014). https://doi.org/10.1039/c3nr06092f

[S3] X. Lei, X. R. Zhang, A. R. Song, S. Gong, Y. Wang et al., Investigation of electrical conductivity and electromagnetic interference shielding performance of Au@CNT/sodium alginate/polydimethylsiloxane flexible composite. Composites, Part A **130**, 105762 (2020). https://doi.org/10.1016/j.compositesa.2019.105762

[S4] J. P. Zhang, H. T. Li, T. Xu, J. J. Wu, S. L. Zhou et al., Homogeneous silver nanoparticles decorating 3D carbon nanotube sponges as flexible high-performance electromagnetic shielding composite materials. Carbon **165**, 404-411 (2020). https://doi.org/10.1016/j.carbon.2020.04.043

[S5] J. H. Cai, X. H. Tang, X. D. Chen, M. Wang, Temperature and strain-induced tunable electromagnetic interference shielding in polydimethylsiloxane/multi-walled carbon nanotube composites with temperature-sensitive microspheres. Composites, Part A. **140**, 106188 (2021). https://doi.org/10.1016/j.compositesa.2020.106188

[S6] Z. Wang, W. Yang, R. Liu, X. Zhang, H. Nie et al., Highly stretchable graphene/polydimethylsiloxane composite lattices with tailored structure for strain-tolerant EMI shielding performance. Compos. Sci. Technol. **206**, 108652 (2021). https://doi.org/10.1016/j.compscitech.2021.108652

[S7] F. Zhang, C. Li, Y. Zhang, Y. Sun, X. Yao et al., Facile preparation of large-scale expanded graphite/polydimethylsiloxane composites for Highly-efficient electromagnetic interference shielding. J Mater. Chem. A (2022). https://doi.org/10.1039/d2ta06263a

[S8] V. T. Nguyen, B. K. Min, Y. Yi, S. J. Kim, C. G. Choi, MXene($Ti_3C_2T_X$)/graphene/PDMS composites for multifunctional broadband electromagnetic interference shielding skins. Chem. Eng. J. **393**, 124608 (2020). https://doi.org/10.1016/j.cej.2020.124608

[S9] S. Kuester, N. R. Demarquette, J. C. Ferreira, B. G. Soares, G. M. O. Barra, Hybrid nanocomposites of thermoplastic elastomer and carbon nanoadditives for electromagnetic shielding. Eur. Polym. J. **88**, 328-339 (2017). https://doi.org/10.1016/j.eurpolymj.2017.01.023

[S10] Y. Xu, S. Tang, J. Pan, J. Bao, A. Zhang, Reversibly cross-linked SEBS/carbon hybrid composite with excellent solvent-proof and electromagnetic shielding properties. Mater. Des. **146**(1-11 (2018). https://doi.org/10.1016/j.matdes.2018.02.071

[S11] Z. Zeng, H. Jin, M. Chen, W. Li, L. Zhou et al., Lightweight and anisotropic porous mwcnt/wpu composites for ultrahigh performance electromagnetic interference shielding. Adv. Funct. Mater. **26**(2), 303-310 (2016). https://doi.org/10.1002/adfm.201503579

[S12] K. Zhang, H.-O. Yu, K.-X. Yu, Y. Gao, M. Wang et al., A facile approach to constructing efficiently segregated conductive networks in poly(lactic acid)/silver nanocomposites via silver plating on microfibers for electromagnetic interference shielding. Compos. Sci. Technol. **156**, 136-143 (2018). https://doi.org/10.1016/j.compscitech.2017.12.037

[S13] J. J. Ju, T. R. Kuang, X. P. Ke, M. Zeng, Z. Chen et al., Lightweight multifunctional polypropylene/carbon nanotubes/carbon black nanocomposite foams with segregated structure, ultralow percolation threshold and enhanced electromagnetic interference shielding performance. Compos. Sci. Technol. **193**, 108116 (2020). https://doi.org/10.1016/j.compscitech.2020.108116

[S14] A. Sheng, W. Ren, Y. Yang, D.-X. Yan, H. Duan et al., Multilayer WPU conductive composites with controllable electro-magnetic gradient for absorption-dominated electromagnetic interference shielding. Composites, Part A. **129**, 105692 (2020). https://doi.org/10.1016/j.compositesa.2019.105692

[S15] R. S. Li, L. Ding, Q. Gao, H. M. Zhang, D. Zeng et al., Tuning of anisotropic electrical conductivity and enhancement of EMI shielding of polymer composite foam via CO_2-assisted delamination and orientation of MXene. Chem. Eng. J. **415**, 128930 (2021). https://doi.org/10.1016/j.cej.2021.128930

[S16] A. P. Singh, M. Mishra, P. Sambyal, B. K. Gupta, B. P. Singh et al., Encapsulation of γ-Fe_2O_3 decorated reduced graphene oxide in polyaniline core–shell tubes as an exceptional tracker for electromagnetic environmental pollution. J Mater. Chem. A **2**(10), 3581-3593 (2014). https://doi.org/10.1039/c3ta14212d

[S17] K. Rajavel, Y. G. Hu, P. L. Zhu, R. Sun, C. P. Wong, MXene/metal oxides-Ag ternary nanostructures for electromagnetic interference shielding. Chem. Eng. J. **399**, 125791 (2020). https://doi.org/10.1016/j.cej.2020.125791

[S18] X. T. Yang, S. G. Fan, Y. Li, Y. Q. Guo, Y. G. Li et al., Synchronously improved electromagnetic interference shielding and thermal conductivity for epoxy nanocomposites by constructing 3D copper nanowires/thermally annealed graphene aerogel framework. Composites, Part A **128**, 105670 (2020). https://doi.org/10.1016/j.compositesa.2019.105670

[S19] N. Bagotia, V. Choudhary, D. K. Sharma, Synergistic effect of graphene/multiwalled carbon nanotube hybrid fillers on mechanical, electrical and EMI shielding properties of polycarbonate/ethylene methyl acrylate nanocomposites. Composites, Part B **159**, 378-388 (2019). https://doi.org/10.1016/j.compositesb.2018.10.009

[S20] I. Arief, S. Biswas, S. Bose, FeCo-anchored reduced graphene oxide framework-based soft composites containing carbon nanotubes as highly efficient microwave absorbers with excellent heat dissipation ability. ACS Appl. Mater. Interfaces **9**(22), 19202-19214 (2017). https://doi.org/10.1021/acsami.7b04053

[S21] H. J. Duan, P. Y. He, H. X. Zhu, Y. Q. Yang, G. Z. Zhao et al., Constructing 3D carbon-metal hybrid conductive network in polymer for ultra-efficient electromagnetic interference shielding. Composites, Part B **212**(108690 (2021). https://doi.org/10.1016/j.compositesb.2021.108690

[S22] M. Sang, Y. X. Wu, S. Liu, L. F. Bai, S. Wang et al., Flexible and lightweight melamine sponge/MXene/polyborosiloxane (MSMP) hybrid structure for high-performance electromagnetic interference shielding and anti-impact safe-guarding. Composites, Part B **211**, 108669 (2021). https://doi.org/10.1016/j.compositesb.2021.108669

[S23] G. Sang, P. Xu, T. Yan, V. Murugadoss, N. Naik et al., Interface Engineered Microcellular Magnetic Conductive Polyurethane Nanocomposite Foams for Electromagnetic Interference Shielding. Nano-Micro Lett. **13**(1), 153 (2021). https://doi.org/10.1007/s40820-021-00677-5

[S24] B. Zhao, S. Wang, C. Zhao, R. Li, S. M. Hamidinejad et al., Synergism between carbon materials and Ni chains in flexible poly(vinylidene fluoride) composite films with high heat dissipation to improve electromagnetic shielding properties. Carbon **127**, 469-478 (2018). https://doi.org/10.1016/j.carbon.2017.11.032

[S25] H. Zhang, G. Zhang, M. Tang, L. Zhou, J. Li et al., Synergistic effect of carbon nanotube and graphene nanoplates on the mechanical, electrical and electromagnetic interference shielding properties of polymer composites and polymer composite foams. Chem. Eng. J. **353**, 381-393 (2018). https://doi.org/10.1016/j.cej.2018.07.144

[S26] B. Yao, W. Hong, T. Chen, Z. Han, X. Xu et al., Highly Stretchable Polymer Composite with Strain-Enhanced Electromagnetic Interference Shielding Effectiveness. Adv. Mater. **32**(14), e1907499 (2020). https://doi.org/10.1002/adma.201907499